J Clust Sci (2017) 28:119–132
DOI 10.1007/s10876-016-1051-6

ORIGINAL PAPER

Eco-friendly Synthesis of Gold Nanoparticles and Evaluation of Their Cytotoxic Activity on Cancer Cells

Maheshkumar Prakash Patil[1] · Daniel Ngabire[1] · Hai Ha Pham Thi[1] · Min-Do Kim[2,3] · Gun-Do Kim[1]

Received: 28 June 2016 / Published online: 25 July 2016

Abstract We herein present a simple, clean, eco-friendly and inexpensive method for green synthesis of gold nanoparticles (AuNPs) using water extract from galls of *Rhus chinensis*. In this study, the reactions were conducted at 50 °C for 15 min using a magnetic stirrer and water as a solvent. AuNP characterization was performed using ultraviolet–visible (UV–vis) spectroscopy, transmission electron microscopy, field-emission scanning electron microscopy, and X-ray diffraction analysis. Element composition was detected via energy dispersive X-ray analysis. The possible presence of functional groups was analyzed using Fourier-transform infrared spectroscopy. The synthesized AuNPs exhibited a color change to wine red and a UV–vis peak at 532 nm. The sizes of AuNPs ranged from 20 to 40 nm, and they had oval and spherical shapes. The cytotoxic effects against MKN-28 (Adenocarcinoma), Hep3B (Heptocellular carcinoma), and MG-63 (Osteosarcoma) cells were evaluated using tetrazolium-based assay. The AuNPs induced cytotoxicity in a dose-dependent manner, and morphology upon cell death was differentiated via fluorescent microscopy using 4,6-Diamidino-2-pheynylindole dihydrochloridehydrate staining which predicted apoptosis.

Keywords Cancer cells · Galls · Gold nanoparticles · Green synthesis · *Rhus chinensis*

✉ Gun-Do Kim
gundokim@pknu.ac.kr

[1] Department of Microbiology, College of Natural Sciences, Pukyong National University, 45 Yongso-ro, Nam-gu, Busan 48513, Republic of Korea

[2] Department of Convergence Medical Science, Graduate School of Inter-departmental Programs, Gyeongsang National University, 501 Jinju-daero, Jinju 52727, Republic of Korea

[3] Institute of Health Science, Gyeongsang National University, 501 Jinju-daero, Jinju 52727, Republic of Korea

Introduction

Nanotechnology is a fast-growing interdisciplinary field with extensive applications in science and technology [1]. Currently, nanotechnology is attractive because it can be employed to biosynthesize novel metals such as gold, silver, copper, platinum, zinc, and titanium nanoparticles using extracts from plant parts such as leaves, fruits, seeds, and peels [2, 3], and because of their pharmacological properties, including anti-microbial, antiviral, antidiabetic, anticancer, and antioxidant properties [4, 5]. Biosynthesized metal nanoparticles have recently been attention because of their advanced biomedical applications such as drug delivery, hypothermal therapy, biosensors, imaging and diagnosis [6], Furthermore, nanoparticles are valuable in therapeutics because of their nano sizes and surface to volume ratios, which significantly improve their chemical and physical properties [7].

Physical and chemical methods of nanoparticle synthesis are harmful to the environment and human beings because of the utilization of hazardous chemicals and high temperatures and pressures [8]; thus, a simple, eco-friendly nanoparticle synthesis method must be developed [9]. Monodispersive gold nanoparticles (AuNPs) are commonly synthesized using citrate as a reducing agent [10]. Moreover, plant extract mediated nanoparticles varying in shape and size because of the presence of multiple reducing agents in plant extracts have been developed [4]. Recently, AuNP biosyntheses using bacteria *Nocardiopsis* sp. and *Brevibacterium casei* [11, 12]; fungus [13]; blue green algae [14]; and plant parts such as leaves [15, 16], stems [16], bark [17], seeds [18], fruits and peels [19, 20], pods [21], roots [22], and gum [23] were reported.

Various types of AuNPs for different purposes and new applications are expected to be developed further. The wide range of nanoparticle applications raises practical concerns about the health effects due to long term exposure. Hence it is necessary to investigate the toxicological effects of nanoparticle exposure. Recent studies that demonstrate the toxic effects of nanoparticles have created controversy [24]. The toxicity of AuNPs depends on the presence of different cell lines and the accumulation of nanoparticles [24, 25]. In addition, several mammalian cell lines showing cytotoxicity induced based on AuNPs aggregation and size dependent [26, 27]. Phytogenic synthesized AuNPs have exhibited a wide range of anticancer effects on several types of cell lines [28, 29].

Cancer is a public health problem worldwide and has a high fatality rate. Treatment of cancer is possible by finding and developing new therapies and techniques. Intelligently designed nanoparticles are exceptionally promising as cancer therapy agents. The natural sources mediated nanoparticles are also used as a nanodrug for controlling mosquito-borne diseases and cancer [30]. AuNPs are useful in this regard for several reasons. First, AuNPs synthesis is simple, and has a high affinity of binding and its conjugation with biomolecules such as DNA, protein, and receptors [31, 32]. AuNPs are also useful tools in specific gene and drug delivery systems [33].

The galls of *Rhus chinensis* is a medicinally important shrub and belongs to the family Anacardiaceae, genus *Rhus,* which contains 250 individual species of

flowering dioecious plants with grown heights of approximately 8 m [34]. This shrub is widely grown in China, India, Taiwan, Japan, and Malaysia. The galls of *R. chinensis* have significant medicinal properties, including anticancer, antioxidant, anti-inflammation, antimicrobial, antiviral, and antidiarrheal properties [35, 36]. Gall formation on *R. chinensis* plant results from an infection caused by Chinese aphids (*Schlechtendalia chinensis*). Galls are rich in hydrolysable tannins and gallotannins [37], and also contains methyl gallate and gallic acid [38]. Synthesis of silver nanoparticles using *R. chinensis* gall extract has been reported in [39].

In this study we utilized a simple, eco-friendly approach for the green synthesis of AuNPs in aqueous solution using a medicinally important *R. chinensis* galls extract (GRC). The characterization was performed using ultraviolet visible (UV–vis) spectroscopy, field-emission scanning electron microscopy (FE-SEM), transmission electron microscopy (TEM), X-ray diffraction (XRD), and energy dispersive X-ray (EDX) analysis. The possible presence of functional groups was analyzed via Fourier transform infrared spectroscopy (FT-IR). The synthesized AuNPs were evaluated for their cytotoxic activities against MKN-28 (stomach; adenocarcinoma), Hep3B (liver; heptocellular carcinoma), and MG-63 (bone/calvaria; osteosarcoma) cells using a tetrazolium-based assay. The nuclear morphologies of cancer cells in treated and non-treated cells were characterized using 4,6-Diamidino-2-pheynylindole dihydrochloridehydrate (DAPI) staining.

Materials and Methods

Materials

Gold (III) chloride trihydrate ($HAuCl_4.3H_2O$) and fetal bovine serum (FBS) were purchased from Sigma Aldrich (St. Louis, MO, USA). Galls of *R. chinensis* were purchased from Jirisan herb food supplier (Sancheong, Korea). EZ-Cytox Cell Viability Assay Solution (WST-1) was provided by Daeil Lab Service (Seoul, Korea). DAPI was obtained from Toche (Mannheim, Germany). The antibiotics penicillin–streptomycin was purchased from PAA Laboratories GmbH, PA, Austria. Formaldehyde was obtained from JUNSEI Chemicals Japan. The 96-well plate and coverslip bottom dishes were purchased from SPL Life-science, Gyeonggi, Korea.

Preparation of Galls Extract

The *Rhus chinensis* galls extract prepared as per the method employed by Patil et al. [39] with some modifications. In brief, purified water washed galls were air dried and powdered in an electric grinder, and 5 gm of this powder were added to a flask containing 50 ml of purified water. This flask was then hold in a water bath at 70 °C for 2 h. The supernatant was collected by centrifugation at 2500 rpm for 20 min and was then filtered with a 5 μm syringe filter. The prepared aqueous extract was stored in a refrigerator.

Biosynthesis of AuNP

AuNPs synthesis was performed using an aqueous solution of chloroauric acid and aqueous GRC. Chloroauric acid solution sample with volumes of 20 ml and different concentrations (1.0, 0.5, 0.25 and 0.125 mM) were prepared, and 200 µl of GRC was added to each tube. The reaction mixtures were held in a water bath at 50 °C for 15 min with continuous magnetic stirring. After reaction, the AuNPs synthesized from 1.0 mM chloroauric acid were collected by centrifugation at 12,000 rpm for 30 min and unwanted material from the reaction solution was removed by washing the AuNPs several times with sterile purified water. The separated AuNPs were freeze-dried to obtain a powder and were kept at −80 °C for further study. Diagram of the gall extraction, AuNPs synthesis, characterization, and application processes are presented in Scheme 1.

Characterization of AuNP

UV–vis spectroscopic analysis was employed for AuNPs synthesis monitoring and was performed using a UV–visible spectrophotometer (Jasco, Japan, model V-670) with a wavelength range of 300–800 nm. TEM analysis was performed for the synthesized AuNPs, to determine their sizes, shapes, and morphologies. The AuNPs samples were placed on a carbon grid and were dried at room temperature. TEM images were acquired using a Transmission Electron Microscope (120 kV, HITACHI, H7500, Japan). The Powdered AuNPs were placed on specimen stubs with double sided adhesive tape coated with platinum in a sputter coater and were observed under Field-emission scanning electron microscope (JSM-6700F, JEOL,

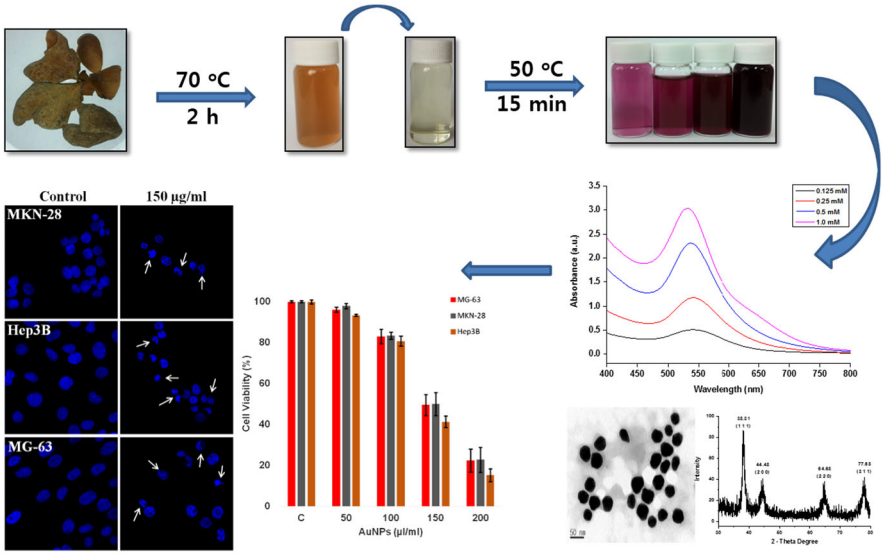

Scheme 1 The diagrammatic representation of AuNPs synthesis process

Japan). In addition, the presence of gold metal was recorded via EDX analysis along with FE-SEM. The freeze-dried AuNPs were utilized for the crystalline structure and diffraction pattern analysis using an X-ray diffractometer (Philips X'Pert-MPD, Netherland) with a 30 mA current and 40 kV voltage in Cu-K α radiation ($\lambda = 1.540$ Å). The presence of a reducing agent in the GRC and the synthesized AuNPs in the GRC were analyzed via FT-IR spectroscopy; GRC and AuNPs were mixed separately in a ratio of 1:100 with dry KBr and thin film palates were prepared. The FT-IR transmittance spectra were measured using an FT-IR spectrometer (Nicolet iS10, Thermo Electron Sci Inst. LLC, WI, USA) with a measurable wavelength range of 400–4000 cm^{-1}.

Cell Culture

MKN-28, Hep3B and MG-63 cells were purchased from the American Tissue Culture Collection (Manassas, VA, USA). The MKN-28 cells were cultured and maintained in the RPMI 1640 medium while; Hep3B and MG-63 were cultured and maintained in Dulbecco's Modified Eagle's Medium. All of the media were supplemented with 10 % FBS, and 1 % streptomycin - penicillin. All of the cultures were incubated at 37 °C with 5 % CO_2.

Antiproliferative Assay

Cancer cells, MKN-28 cells, Hep3B cells, and MG-63 cells were seeded in each well of a 96-well plate at a final concentration of 2×10^5 cells/100 µl and were incubated at 37 °C in 5 % CO_2 for 24 h. After incubation, the cells were treated with different concentrations of AuNPs (50 µg/ml, 100 µg/ml, 150 µg/ml, and 200 µg/ml) and were further incubated for 24 h under the same conditions as mentioned above. After incubation, the media in the wells were replaced by fresh media. Then, a 10 µl aliquot of WST-1 was added to each well, and the 96 wells plate was incubated for an additional 3 h. The optical density (OD) was measured at 460 nm using a Microplate reader (Molecular Devices, Siliconvalley, CA, USA).

$$\text{Cell viability}(\%) = \text{OD of treated cells}/\text{OD of control cells} \times 100 \quad (1)$$

Immunofluorescence Staining

The nuclear morphologies of the cells were evaluated via fluorescence microscopy using DAPI staining. In brief, the MKN-28, Hep3B, and MG-63 cells were seeded at a final concentration 10^4 cells/µl on the coverslip bottom dishes and were incubated for 24 h. After incubation, the cells were treated with or without AuNPs (150 µg/ml) and were incubated for an additional 24 h. After, the cells were washed with phosphate buffer saline (PBS; pH 7.4) DAPI (diluted in methanol) was added to the cells. The dishes were protected from light exposure by wrapping them in aluminum foil, and they were incubated for 15 min at 37 °C. The cells on the coverslips were embedded using prolong

antifade reagent (Invitrogen, Eugene, OR, USA) and nuclear condensation was observed via a Laser Scanning Microscope (CarlZeiss Microscope LSM700, Germany).

Statistical Analysis

The UV–vis spectroscopy and FT-IR graphs were prepared using Origin Pro 9.1 SRO software (OriginLab Corp, USA). All of the cytotoxicity experiments were performed in triplicates, and the results were presented as the mean ± standard deviation (SD). The data were tabulated and analyzed using SPSS statistical software package version 20 and were performed one way ANOVA followed by Tukey's HSD test. The confidence of the study was proposed to be 95 %; hence, a probability level of $P < 0.05$ was used for the significance of differences between values.

Results and Discussion

Characterization of AuNP

Visual Observation

The change in color of chloroauric acid after the addition of a reducing agent is the first sign of AuNPs synthesis [11, 17]. In this study, adding GRC to a chloroauric acid solution resulted in a color change from pale yellow to violet-wine red. Figure 1a depicts the galls utilized in this study, and Fig. 1b shows the GRC and the, 1 mM chloroauric acid solution (reaction controls) in first and second tube, respectively. The color changes from in the 0.125, 0.25, 0.5, and 1 chloroauric acid solutions after their reactions are shown from left to right. The specific colors changed during the reactions because of the formation of AuNPs and the surface plasmon resonance vibrations of the AuNPs that were synthesized in the reaction mixtures [40].

UV–visible Spectrophotometry

AuNPs synthesis was confirmed via UV–vis spectroscopy. Reaction mixtures with volumes of 20 ml and different chloroauric acid concentrations (0.125, 0.25, 0.5, and 1.0) with 200 µl of GRC were analyzed via UV–vis spectroscopy. Figure 1c depicts the UV–vis spectroscopic absorption range from 400 nm to 800 nm and shows a peak at 532 nm for the 1 mM chloroauric acid reaction mixture. The reaction controls (chloroauric acid and GRC alone) were unchanged after the reaction; however, the absorbance increased with increasing chloroauric acid concentration. The absorbance peak at approximately 540 nm is characteristic of AuNPs and has been reported previously [40, 41]. Absorbance depends on chloroauric acid concentration, and the particle size varies [9, 20, 23]. In this study, a 1 mM chloroauric acid reaction mixture was utilized for characterization and the investigated applications.

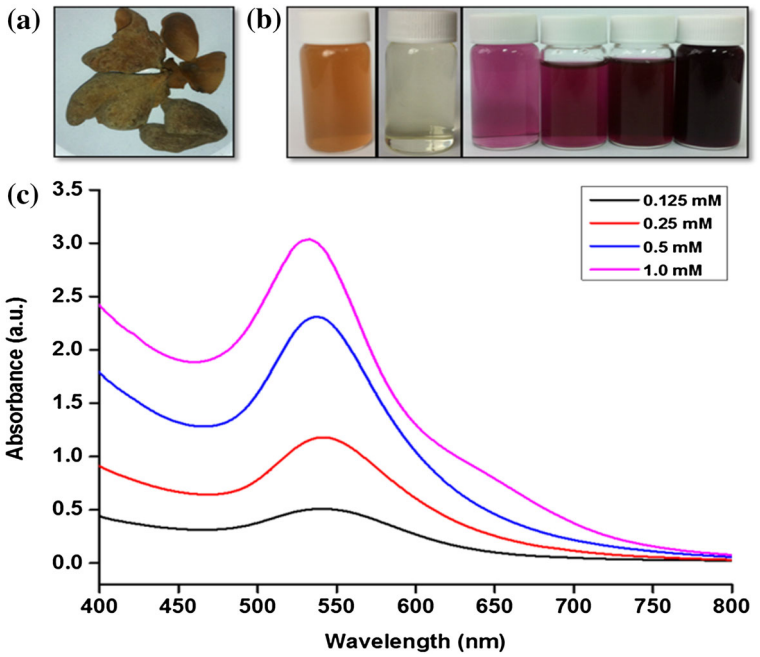

Fig. 1 **a** The Galls of *Rhus chinensis*; GRC. **b** From *left to right*:- GRC extract, 1 mM chloroauric acid solution, reaction tubes with concentrations 0.125, 0.25, 0.5, and 1.0 mM of chloroauric acid. **c** UV–vis spectra of the AuNPs synthesized in different concentrations of chloroauric acid (0.125, 0.25, 0.5, and 1.0 mM) in presence of 1 % GRC extract as the reducing agent and at 50 °C for 15 min incubation

Transmission Electron Microscopy

TEM results confirms the sizes and shapes of the synthesized AuNPs. Figure 2 reveals that the synthesized AuNPs were spherical, oval shaped, and had sizes of 20–40 nm. Irregularly shaped AuNPs were formed because of the presence of more than one reducing agent in the plant extract [2, 41]. Green synthesized AuNPs range in size from 10 to 50 nm. Polymorphic shapes have been reported for different plants [9, 16–20]. The results obtained in the present study are in good agreement with the results obtained for green synthesized AuNPs. To the best of our knowledge, we are the first to report the synthesis of AuNPs using GRC as a reducing agent.

Field-Emission Scanning Electron Microscopy and Energy Dispersive X-ray Analysis

FE-SEM analysis was performed for the freeze dried sample. Its shape and size were determined from the FE-SEM image (Fig. 3a). Its elemental composition was confirmed via EDX and FE-SEM. The EDX analysis result is presented in Fig. 3b. The strong energy peak at 2 keV indicates the presence of gold metal. The typical

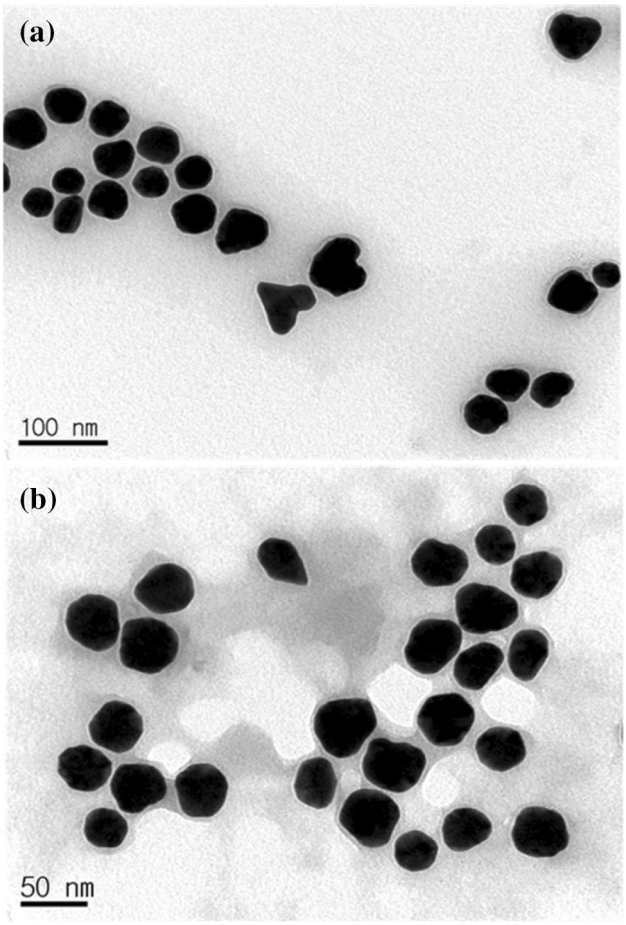

Fig. 2 TEM images illustrating the synthesized AuNPs in GRC extract with scale of **a** 100 nm and **b** 50 nm

absorption peak around 2 keV is characteristic of metallic and gold nano-crystals [20, 22].

X-ray Diffraction Analysis

The XRD diffraction patterns of the synthesized AuNPs are shown in Fig. 4. The diffraction peaks occur at $2\theta = 38.31, 44.48, 64.68$, and 77.68^{o} and were indexed as (111), (200), (220), and (311) planes on the basis of the faced centered cubic structures of AuNPs. The broadening of Bragg's peak indicates the formation of nanoparticles. The present results are in good agreement with those obtained for green synthesized AuNPs [22, 40].

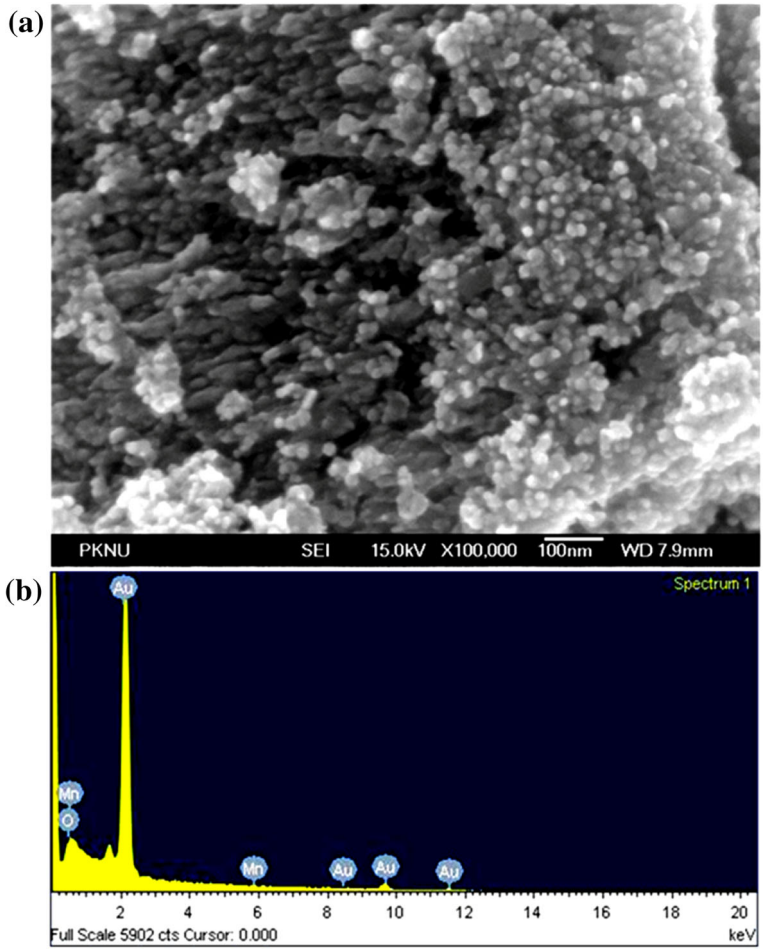

Fig. 3 **a** FE-SEM image of the AuNPs formed by the reaction of 1.0 mM chloroauric acid and 1 % GRC extract and **b** EDX spectrum of the synthesized AuNPs

Fourier Transform Infrared Spectroscopy

The identification and characterization of functional biocompounds present in GRC and the AuNPs synthesized in GRC were analyzed via FT-IR spectroscopy. The FT-IR spectra of GRC and the AuNPs with GRC are depicted in Fig. 5a and b, respectively, and both spectra shows shifts in their peaks and transmittance. For GRC the vibration stretches are observable at 3224 cm^{-1}, 2988, 1705, 1607, 1535, 1445, 1313, 1195, 1083, 1026, 868, and 758 cm^{-1}, and the AuNPs with GRC exhibit peaks at 3239, 2988, 1705, 1603, 1528, 1445, 1326, 1195, 1078, 1051, 880, and 758 cm^{-1}. The band at 3224 cm^{-1} corresponds to the stretching vibration of the hydroxyl group (O–H) of phenol compounds. The peak at 1607 cm^{-1} is due to the N–H bond stretching of the functional groups in amines and the weaker peak at

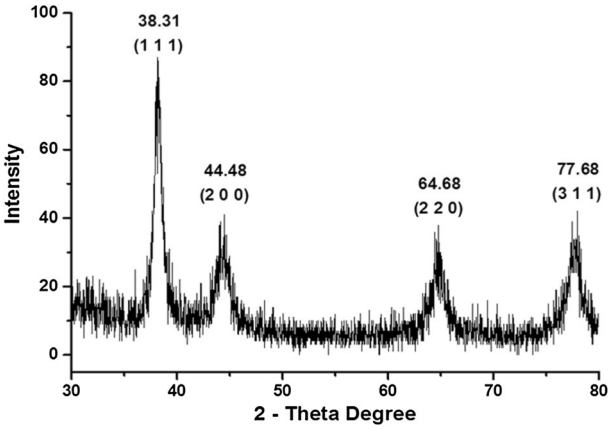

Fig. 4 XRD pattern of the synthesized AuNPs with GRC extract

1535 cm^{-1} corresponds to asymmetric N–O bond stretching and can be assigned to the functional groups in nitrogen compounds. The peaks at 1313 and 1026 cm^{-1} correspond to the C–N bond stretching in the functional groups of aromatic and aliphatic amines, respectively. The medium vibration stretching at 1083 cm^{-1} results from the C–N bonds and can be assigned to the functional groups in esters and ethers. The peak at 868 cm^{-1} corresponds to the = C–H bond stretching and is characteristic of the functional groups in alkenes. In the AuNPs with GRC, the peak shifts from 3224 to 3239 cm^{-1}, 1607 to 1603 cm^{-1}, 1535 to 1528 cm^{-1}, 1313 to 1326 cm^{-1}, 1083 to 1078 cm^{-1}, 1026 to 1051 cm^{-1}, and 868 to 880 cm^{-1} are

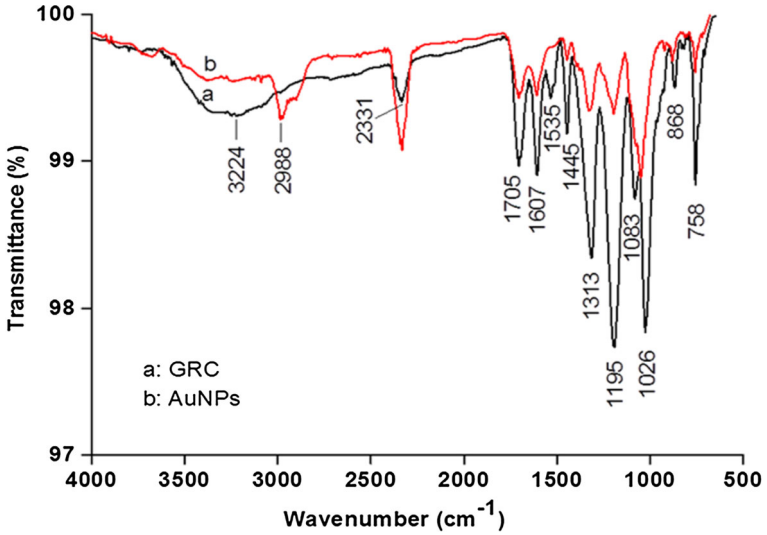

Fig. 5 *a* FT-IR spectra of GRC extract and *b* the synthesized AuNPs with GRC extract

observable; this indicates the reduction of chloroauric acid to AuNPs. The ether and ester functional groups present in gallotannins [37] and aqueous extract of galls are rich in tannins and polyphenols [36]. Various groups have reported the involvement of hydroxyl groups in the AuNP synthesis and that the transmittance variations and peak shifts mainly results from the influence of biocompounds on reduction and capping of nanomaterials [16, 23].

Antiproliferative Assay

AuNPs are attracting increasing interest as novel agents for cancer therapy [28]. There are limited studies on the cytotoxic effects of AuNPs against different cancer cells. WST-1 assay was performed to determine the effects of AuNPs on the proliferation of MKN-28, Hep3B, and MG-63 cell lines. In the present study, we found that the antiproliferative activities of AuNPs may be due to the induction of an apoptosis. Dose dependent cytotoxicity was observed (Fig. 6a) against cancer cells (from ANOVA analysis results; value of $F = 152.527$, 152.954, and 547.338 for the cancer cells MKN-28, MG-63, and Hep3B respectively and $d.f. = 14$, and $P < 0.05$ values similar for all cancer cell lines). The sample with an AuNP concentration of 50 µg/ml was not very active; however, high cytotoxic activity was observed when the 100 µg/ml sample was employed, and the 200 µg/ml sample reduced all of the cells to around 20 % viability. Cell inhibition of 50 % was observed at an AuNPs concentration of approximately 150 µg/ml. The increasing cytotoxicity of AuNPs from MKN-28 to MG-63 to Hep3B was recorded. The cytotoxic effects of the green synthesized AuNPs against different cancer calls [16, 19, 25, 42] are in good agreement the results obtained in this study. Jayaraj

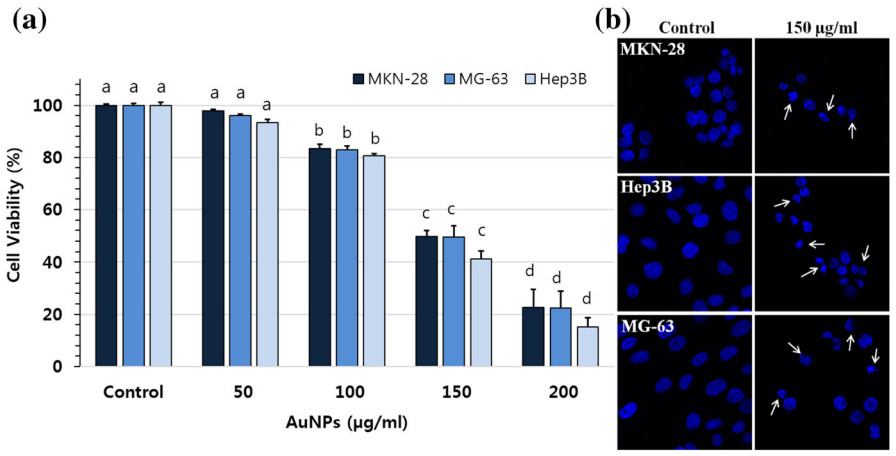

Fig. 6 **a** Histogram of cancer cell viability obtained using the WST-1 method at different AuNPs concentrations and, *Error bars* indicates ± standard deviation (n = 3). *Different letters* above each *column* indicated significant differences among treatment; one way ANOVA, Tukey's HSD test, $P < 0.05$. **b** Results of fluorescence microscopic analysis using DAPI staining for nuclear morphology detection; the *arrow* indicates nuclear fragmentation and condensation

et al. reported the anticancer activity of AuNPs using a G2/M growth phase arrest and concluded that nanoparticles causes DNA damage and caspase dependent apoptosis in HeLa cells [43]. AuNPs are novel agents for cancer therapy [28], and shows aggregations [24], and size dependent cytotoxic activity against different cancer cells [27]. AuNPs are gaining significant attention from researchers because of their biocompatibility and the ability to conjugate with proteins [31].

Immunofluorescence Staining

DAPI staining has been applied to stain nuclei and has also been used to detect nucleus fragmentation [26, 42]. Murugan et al. reported evidence of apoptosis by DNA fragmentation in human breast cancer cells using DAPI staining [44]. DAPI stains interact with nucleotides and emit blue fluorescence. The cells treated and not treated by AuNPs were stained by DAPI; the blue structures represents the nuclei (Fig. 6b). In the immunofluorescence image, intact round or oval shaped nuclei are observable among the non-treated (control) cells, and condensed or fragmented nuclear material (marked by arrows) is observable in the cells treated with AuNPs (150 μg/ml). Nuclear fragmentation and condensation are characteristic features of apoptosis, and AuNP mediated reactive oxygen species are responsible for the DNA damage and apoptosis in cancer cells [6, 26, 42].

Conclusion

To the best of our knowledge this is the first report of using GRC as a reducing and capping agent for successful AuNP synthesis. The synthesized AuNPs was characterized via visual observation, UV–vis spectroscopy, TEM, FE-SEM with EDX, and XRD. Possible functional groups involved in the AuNPs synthesis were detected by FT-IR. The synthesized AuNPs were spherical and oval shaped with sizes ranging 20 to 40 nm. The AuNPs induced cytotoxicity in cancer cells, and the dose-dependent cytotoxic effects against MKN-28, Hep3B, and MG-63 cancer cell lines were observed. Cell inhibition of 50 % was observed when an AuNP solution with a concentration of approximately 150 μg/ml was applied and nuclear fragmentation was observed at the same concentration. Thus, green synthesized AuNPs can be used as therapeutic agents in cancer treatment. A detailed study is needed to understand the mode of action and the mechanism behind the cell death caused by green synthesized AuNPs.

Acknowledgments This study was supported by the research funds provided by the Pukyong National University in 2016.

References

1. M. A. Albrecht, C. W. Evans, and C. R. Raston (2006). *Green Chem.* **8**, 417.
2. R. Mohammadinejad, S. Karimi, S. Iravani, and R. S. Verma (2016). *Green Chem.* **18**, 20.
3. A. K. Mittal, Y. Chist, and U. C. Banerjee (2013). *Biotechnol. Adv.* **31**, 346.

4. P. Kappusamy, M. M. Yusoff, G. P. Maniam, and N. Govindan (2015). *Saudi. Pharm. J*. doi:10.1016/j.jsps.2014.11.013.
5. S. Iravani (2011). *Green Chem.* **13**, 2638.
6. F. S. Rosarin and S. J. Mirunalini (2011). *J. Bioanal. Biomed.* **3**, 85.
7. V. P. Zharov, J. W. Kim, D. T. Curiel, and M. Everts (2005). *J. Nanomed. Nanotechnol.* **1**, 326.
8. N. Sharma, G. Bhatt, and P. Kothiyal (2015). *Indian. J. Pharm. Biol. Res.* **3**, 13.
9. M. Shah, D. Fawcett, S. Sharma, S. K. Tripathy, and G. E. J. Poinern (2015). *Materials* **8**, 7278.
10. H. Hiramatsu and F. E. Osterloh (2004). *Chem. Mater.* **16**, 2509.
11. P. Manivasagan, M. S. Alam, K. H. Kang, M. Kwak, and S. K. Kim (2015). *Bioprocess. Biosyst. Eng.* **38**, 1167.
12. K. Kalishwaralal, V. Deepak, S. R. K. Pandian, M. Kottaisamy, S. Barathmanikanth, B. Kartikeyan, and S. Gurunathan (2010). *Colloids surf. B Biointerfaces.* **77**, 257.
13. A. Chauhan, S. Zubair, A. Sherwani, M. Sajid, S. C. Raman, A. Azam, and M. Owais (2011). *Int. J. Nanomedicine.* **6**, 2305.
14. K. S. U. Suganya, K. Govindraju, V. G. Kumar, T. S. Dhas, V. Karthick, G. Singarasvelu, and M. Elanchezhiyan (2015). *Mater. Sci. Eng. C.* **47**, 351.
15. C. Tiloke, A. Phulukdaree, K. Anand, R. M. Gengan, and A. A. Chuturgoon (2016). *J. Cell. Biochem.* doi:10.1002/jcb.25528.
16. P. Mishra, S. Ray, S. Sinha, B. Das, M. I. Khan, K. B. Behera, S. I. Yun, S. K. Tripathy, and A. Mishra (2015). *Biochem. Eng. J.* **105**, 264.
17. R. Majumdar, B. G. Bag, and P. Ghosh (2015). *Appl. Nanosci*. doi:10.1007/s13204-015-0454-2.
18. S. A. Aromal and D. Philip (2012). *Spectrochim. Acta. A Mol. Biomol. Spectrosc.* **97**, 1.
19. B. Kumar, K. Smita, L. Cumbal, J. Camacho, E. Hernandez-Gallegos, M. D. G. Chavez-Lopez, M. Grijalva, and K. Andrade (2016). *Mater. Sci. Eng. C.* **62**, 725.
20. A. Bankar, B. Joshi, A. R. Kumar, and S. Zinjarde (2010). *Colloids surf. B Biointerfaces.* **80**, 45.
21. M. Pattanayak and P. L. Nayak (2013). *World J. NanoSci. Technology.* **2**, 01.
22. T. Y. Suman, S. R. Radhika Rajasree, R. Ramkumar, C. Rajthilak, P. Perumal (2014). *Spectrochim. Acta. A*. **118**, 11.
23. G. B. Reddy, A. Madhusudhan, D. Ramakrishna, D. Ayodhya, M. Venkateshan, and G. Veerabhadram (2015). *J. Nanostruct. Chem.* **5**, 185.
24. W. Cui, J. Li, Y. Zhang, H. Rong, W. Lu, and L. Jiang (2012). *Nanomedicine* **8**, 46.
25. P. J. Chueh, R. Y. Liang, Y. H. Lee, Z. M. Zeng, and S. M. Chuang (2014). *J. Hazard. Mater.* **264**, 303.
26. R. Coradeghini, S. Gioria, C. P. Garcia, P. Nativo, F. Franchini, D. Gilliland, J. Ponti, and F. Rossi (2013). *Toxicol. Lett.* **217**, 205.
27. Y. Pan, S. Neuss, A. Leifert, M. Fischler, F. Wen, U. Simon, G. Schmid, W. Brandau, and W. Jahnen-Dechent (2007). *Small* **3**, 1941.
28. S. Jain, D. G. Hirst, and J. M. O'Sulliva (2012). *Br. J. Radiol.* **85**, 101.
29. S. M. Faheem and B. Hussaina (2014). *Austin J. Biotechnol. Bioeng.* **1**, 5.
30. G. Benelli, A. L. Iacono, A. Canale, and H. Mehlhorn (2016). *Parasitol. Res.* **115**, 2131.
31. P. Wang, X. Wang, L. Wang, X. Hou, W. Liu, and C. Chen (2015). *Sci. Technol. adv. mater*. doi:10.1088/1468-6996/16/3/034610.
32. J. Fang, L. Yu, P. Gao, Y. Cai, and Y. Wei (2010). *Anal. Biochem.* **399**, 262.
33. D. Pissuwan, T. Niidome, and M. B. Cortie (2011). *J. Control. Release.* **149**, 65.
34. A. J. Miller, D. A. Young, and J. Wen (2001). *Int. J Plant Sci.* **162**, 1401.
35. O. Djakpo and Y. Weirong (2010). *Phytother.Res.* **24**, 1739.
36. F. Tian, B. Li, B. Ji, J. Yang, G. Zhang, Y. Chen, and Y. Luo (2009). *Food Chem.* **113**, 173.
37. C. H. Kee, M. W. Walter. The Pharmacology of Chinese Herbs, 2nd edn. (CRC press LLC, Boca Raton (1999), pp 239.
38. I. S. Buziashvii, N. F. Komissarenko, I. P. Kovalev, V. G. Gordienko, and D. G. Kolesnikov (1973). *Chem. Nat. Compd.* **9**, 752.
39. M. P. Patil, A. A. Rokade, D. Ngabire, and G-D. Kim (2016). *J. Clust. Sci*. doi:10.1007/s10876-016-1037-4.
40. U. I. Islam, K. Jalil, M. Shahid, A. Rauf, N. Muhammad, A. Khan, M. R. Shah, and M. A. Khan (2015). *Arab. J. Chem.* doi:10.1016/j.arabjc.2015.06.025.
41. P. Elia, R. Zach, S. Hazan, S. Kolusheva, Z. Porat, and Y. Zeiri (2014). *Int. J. Nanomedicine.* **9**, 4007.
42. R. Geetha, T. Ashokkumar, S. Tamilselvan, K. Govindaraju, M. Sadiq, and G. Singaravedu (2013). *Cancer Nano.* **4**, 91.

43. M. Jayaraj, R. Arun, G. Sathishkumar, D. MubarakAli, M. Rajesh, G. Sivanandhan, G. Kapildev, M. Manickavasagam, N. Thajuddin, and A. Ganapathi (2014). *Mater. Res. Bull.* **52**, 15.
44. K. Murugan, D. Dinesh, K. Kavithaa, M. Paulpandi, T. Ponraj, M. S. Alsalhi, S. Devanesan, J. Subramaniam, R. Rajaganesh, H. Wei, S. Kumar, M. Nicoletti, and G. Benelli (2016). *Parasitol. Res.* **115**, 1085.